Modulatory Effect of Low-Intensity Transcranial Ultrasound Stimulation on Behaviour and Neural Oscillation in Mouse Models of Alzheimer's Disease

Huifang Yang, Jiaqing Yan, Hui Ji, Mengran Wang, Teng Wang, Huiling Yi, Lanxiang Liu, Xin Li, and Yi Yuan

***Abstract*— Transcranial ultrasound stimulation (TUS) is a noninvasive brain neuromodulation technique. The application of TUS for Alzheimer's disease (AD) therapy has not been widely studied. In this study, a long-term course (28 days) of TUS was used to stimulate the hippocampus of APP/PS1 mice. We examined the modulatory effect of TUS on behavior and neural oscillation in AD mice. We found that TUS can 1) improve the learning and memory abilities of AD mice; 2) reduce the phase-amplitude coupling of delta-epsilon, delta-gamma and theta-gamma frequency bands of local field potential, and increase the relative power of epsilon frequency bands in AD mice; 3) reduce the spike firing rate of interneurons and inhibit the phase-locked angle deflection between the theta frequency bands and the spikes of the two types of neurons that develops with the progression of the disease in AD mice. In summary, we demonstrate that TUS could effectively improve cognitive behavior and modulate neural oscillation with AD.**

***Index Terms*— Alzheimer's disease, behaviour, neural oscillation, transcranial ultrasound stimulation.**

Manuscript received 3 July 2023; revised 10 December 2023 and 7 January 2024; accepted 3 February 2024. Date of publication 8 February 2024; date of current version 15 February 2024. This work was supported in part by the National Natural Science Foundation of China under Grant 62273291, Grant 62394310, Grant 62394313, and Grant 62394314; in part by the Natural Science Foundation of Hebei Province under Grant F2022203050 and Grant F2022203005; in part by the Medical–Industrial Crossover Special Incubation Project of Yanshan University and the First Hospital of Qinhuangdao under Grant UY202201; and in part by the Hebei Province Central Guide Local Science and Technology Development Fund Project under Grant 236Z7703G. *(Corresponding authors: Xin Li; Yi Yuan.)*

This work involved animals in its research. Approval of all ethical and experimental procedures and protocols were granted by the Animal Ethics and Administrative Council of Yanshan University.

Huifang Yang, Mengran Wang, Teng Wang, Xin Li, and Yi Yuan are with the Institute of Electrical Engineering, Yanshan University, Qinhuangdao 066004, China (e-mail: yddylixin@ysu.edu.cn; yuanyi513@ysu.edu.cn).

Jiaqing Yan is with the College of Electrical and Control Engineering, North China University of Technology, Beijing 100041, China.

Hui Ji is with the Department of Neurology, Second Hospital of Hebei Medical University, Shijiazhuang 050000, China.

Huiling Yi and Lanxiang Liu are with the Department of Magnetic Resonance Imaging, Qinhuangdao Municipal No. 1 Hospital, Qinhuangdao 066002, China.

This article has supplementary downloadable material available at https://doi.org/10.1109/TNSRE.2024.3363912, provided by the authors.

Digital Object Identifier 10.1109/TNSRE.2024.3363912

I. Introduction

ALZHEIMER'S disease (AD) is the most common neurodegenerative disease [1]. Current treatments for AD include drug therapy and physical intervention. Drug therapy, for which the most commonly used agents are cholinesterase inhibitors and antioxidants, can improve the symptoms of AD patients, reduce the loss of cognitive and functional abilities, preserve the functional level of AD patients to the greatest extent possible, delay the progression of the disease, and improve patients' life expectancy and quality of life [2]. Noninvasive physical brain stimulation therapy includes transcranial magnetic stimulation (TMS) and transcranial direct current stimulation (tDCS). Low-frequency repetitive TMS can enhance the learning and memory ability of AD rats and effectively improve the symptoms of AD patients by regulating the excitability of the cerebral cortex, remodelling the cortical neural network, and increasing the expression of the neurotrophic factor brain-derived neurotrophic factor (BDNF) and the receptors for various ligands [3], [4]. tDCS can regulate the excitability of the cortex and produce long-term effects, which can effectively alleviate the cognitive impairment of AD patients and improve memory and cognitive function [5].However, TMS and tDCS have shortcomings in penetration depth, for instance, they cannot stimulate deep brain areas such as the thalamus [6]. In recent years, transcranial ultrasound stimulation (TUS) with non-invasive, high penetration depth and high spatial resolution has attracted the attention of many scholars and been used in neuromodulation of AD.

Ultrasound wave which consists of propagating waves with a frequency higher than the audible range, can penetrate biological tissues such as the skull and stimulate deep target regions. TUS has the advantages of noninvasiveness, deep penetration of tissue, and high spatial resolution [7], [8], [9], [10], [11], [12]. In general, TUS regulates nerve function through biophysical effects on targets such as mechanosensitive ion channels, glial cells, and cell membrane capacitance [13], [14]. In research on the treatment of Alzheimer's disease by ultrasound, Park et al. applied gamma-frequency (40 Hz) ultrasound to 5XFAD mice for two hours daily for two consecutive weeks and found that transcranial ultrasound

with gamma-frequency ultrasound can effectively treat AD by reducing the amyloid-β (Aβ) load and improving brain connectivity [15]. In the APP23 mouse model of AD, transcranial ultrasound combined with intravenous injection of microbubbles has been shown to temporarily open the blood?brain barrier and reduce Aβ, which highlights the complexity of the microglial response to transcranial ultrasound and its potential application in the treatment of AD [16]. Studies have also shown that TUS has a significant effect on brain damage and cognition in an $AlCl_3$-induced rat model of Alzheimer's disease [17]. The above results suggest that ultrasound stimulation has the potential to be an effective and noninvasive treatment for AD. The APP/PS1 AD mouse model used in this article carries mutated APP and PS1 genes. With the accumulation of gene effects, typical features similar to AD can appear in pathology and learning cognitive abilities, effectively simulating the characteristics of AD. Many scholars have studied the treatment and pathogenesis of AD based on this model mouse, which has high application value [18], [19], [20]. However, it remains unclear how long-term low-intensity TUS modulates neural activity in the hippocampal brain region, which is closely related to learning and memory, of the APP/PS1 AD mouse model.

To answer this question, we used a long-term course (28 days) of low-intensity TUS to stimulate the hippocampus of AD mice. Based on the improvement in AD-related behaviours after ultrasound stimulation, the average relative power and cross-frequency phase-amplitude coupling of different rhythms in the hippocampus during ultrasound stimulation were analysed. Moreover, the spike firing rates of different types of neurons and the phase-locked relationship of their single spikes and theta rhythms were quantified and calculated to further clarify the modulatory effect of long-term low-intensity TUS on neural activity in the hippocampus of the APP/PS1 AD mouse model.

II. Materials and Methods

A. Animal Preparation

Our study protocols were submitted to and approved by the Animal Ethics and Administrative Council of Yanshan University.In this study, twelve female C57BL/6 mice (ages: 12-16 weeks, weight: 20-25 g, Beijing Vital River Laboratory Animal Technology Co., Ltd. China) were used as the Control group. Additionally, twenty-four female APP/PS1 transgenic mice (ages: 12-16 weeks, weight: 20-25 g, Beijing HFK Bio-Technology Co., Ltd. China) were randomly divided into an AD group (N=12) and an ADsti group (N=12), for which female APP/PS1 mice show earlier and higher β amyloid plaque load and earlier memory deficits compared to age-matched males [21], [22]. The Control group, AD group and ADsti group were randomly divided into two subsets for behavioural experiments and electroencephalogram (EEG) recording. What's more, 6 female APP/PS1 transgenic mice were applied with trapezoidal pulses to prove auditory response. All animals were kept in an animal housing room on a 12 h/12 h light/dark cycle; the temperature and humidity were controlled at 20-24 °C and 45%-55%, respectively, and the mice had unrestricted access to standard pelleted rodent feed and water.

5xFAD is a new type of AD mouse model developed on the basis of APP/PS1 and has received widespread attention. In recent animal studies on AD, APP/PS1 mice was widely used as the AD model due to that they have the characteristics of AD well at the cellular and molecular levels [18], [19], [20]. We believe that APP/PS1 mice can meet our study. The APP/PS1 mice used in our study were heterozygous and the company provided corresponding genetic testing reports to ensure that the mice contain characteristic genes.

B. TUS Therapy

The TUS setup was similar to that used in our previous study (Fig. 1a-left) [12]. Ultrasound treatment was performed with a 0.5-MHz unfocused piezoelectric transducer (V301-SU, Olympus, United States) with a 50-msec burst at a 5% duty cycle and a repetition frequency of 1 Hz (Fig. 1c). In our experimental setup, we adjusted the transducer position by integrating the sound field distribution with the mouse brain atlas to make the maximum ultrasound intensity target the hippocampus. The ultrasound intensity distribution under the ex vivo mouse skull in the x-y plane (Fig. 1e) and the normalized amplitude for 1 (Fig. 1d) were measured with a calibrated needle-type hydrophone (HNR500; Onda, United States) that was moved by a two-dimensional electric translation platform. The diameter of the focal area measured at full width at 50% maximum was ∼6.2 mm (Fig. 1d). The head of mouse was shaved, and low-intensity TUS was applied to the hippocampus of the ADsti group vertically only for a sonication time of 15 min at an ultrasound intensity of 0.3 MPa (corresponding to a spatial peak pulse average intensity (I_{SPPA}) of 6 W/cm^2) daily for a period of 28 days (Fig. 1b).In our study, the mice were anesthetized by the isoflurane only during the ultrasound stimulation. Because the mice from all groups underwent the same anesthesia procedure, the statistical differences in experimental results between groups were due to ultrasound stimulation.

C. Experimental Procedures

In this study, a long-term course of ultrasonic stimulation (15 minutes per day for 28 days) was applied to the hippocampus of APP/PS1 mice, and behavioural experiments, EEG recordings and biochemical tests were carried out. We know that AD shows symptoms such as memory impairment, and the hippocampus is closely related to the memory. Therefore, the hippocampus was chosen as the stimulation site in our study [23], [24]. AD is a chronic neurodegenerative diseases and long-term TUS pattern may be more appropriate. In previous studies, 2-weeks period of ultrasound stimulation was used in vascular dementia rats and 6-weeks period of ultrasound stimulation was applied on aluminum induced AD models, which achieved effective stimulation effects [17], [25]. We referred to the previous studies and selected 4-weeks as the stimulation cycle.The timeline of the experiment is shown in Figure 1b which does not include the training period of the fear conditioning test. Ultrasound stimulation for the ADsti group was given daily on D0-D27. In addition, the fear

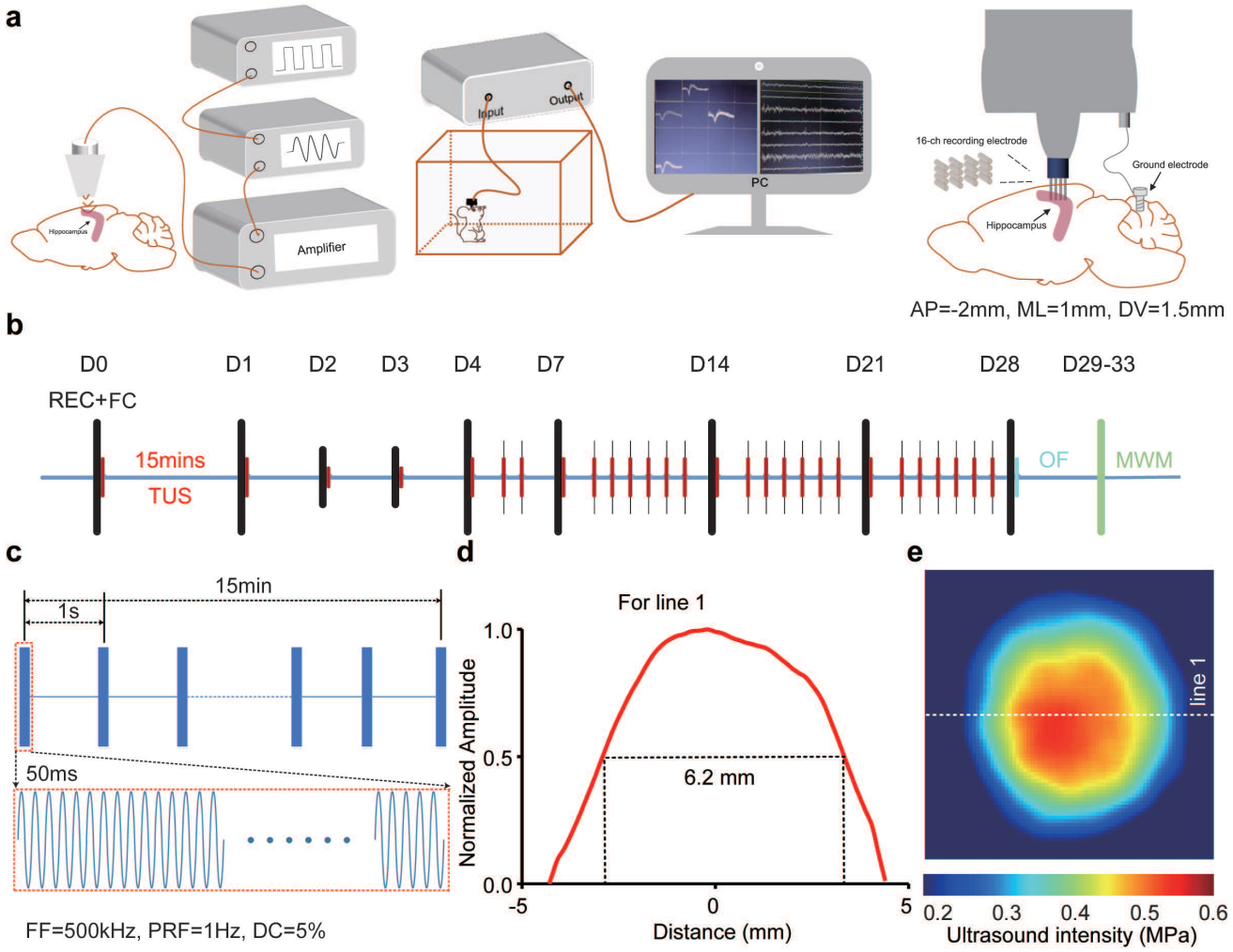

Fig. 1. Experimental setup and protocol. (a) Schematic of ultrasound stimulation (left), electroencephalogram (EEG) recording (middle) and electrode implantation (right). (b) The timeline of the experiment. (c) Time sequence of the imaging experiments. FF: fundamental frequency; PRF: pulse repetition frequency; NC: number of cycles, DC: duty cycle. (d) The reconstruction profile along white dotted line 1 in Figure 1(e). (e) Ultrasound field distribution under the skull in the x-y plane. Abbreviations:FC, fear conditioning test; MWM, Morris water maze; OF, Open field; REC, EEG recording; TUS, Transcranial ultrasound stimulation.

conditioning test and EEG acquisition took place on the same dates, that is, D0-D6, W1 (D7), W2 (D14), W3 (D21), and W4 (D28), which the eleven specific days are collectively referred to as "day collection in stimulation (day CIS)". During day CIS, TUS was performed after the fear conditioning test and EEG acquisition. Subsequently, the open field experiment was carried out on D28, the five-day Morris water maze experiment was carried out on D29-D33.

D. Fear Conditioning

The fear conditioning test is one of the commonly used behavioural research methods to test for cognitive dysfunction in experimental animals [26]. The specific experimental steps are divided into two parts. 1) Establishment of fear memory (training): The mice were trained in the fear box for two days. On the first day, the mice were placed in the fear box to adapt for 150 s, after which sound stimulation (80 dB, 3 600 Hz, for 30 s) was applied 5 times at intervals of 90 s. This part served to verify that mice did not have excessive responses to the sound stimuli before undergoing fear conditioning. On the second day, the other conditions remained unchanged, but a continuous direct current stimulation (current intensity 0.3 mA, duration 0.5 s) was given in the last 0.5 s of the sound stimulation so that the mice developed fear memory for the sound stimulation. 2) The fear conditioning test(testing): After the training, the behavioural performance of the mice after the sound stimulation was recorded during day CIS. The video was recorded by the fear box (Shanghai Jiliang Software Technology Co. Ltd), then the trajectory of each mouse and the immobility time ratio within 150 s after the sound stimulation were quantitatively analysed to evaluate cognitive function.

E. Open Field Test

After 28 days (4 weeks) of ultrasonic stimulation, the open field test was carried out, and the autonomous activity ability and anxiety state of the mice were measured by the open field test [27]. We placed each mouse into the experimental box (50 cm×50 cm) for 10 minutes to adapt before the experiment. We then recorded 3 times for 5 minutes each, separated by intervals of 5 minutes. After each recording, the mice were put back into the cages, and the experimental box was wiped with 75% alcohol to prevent the odour produced by the mice from

affecting the experimental results. Performance was monitored with a video recording system (Basler, acA1280-60gm). After the experiment, quantitative analysis was performed on the motion trajectory, speed, and distance of the mice as well as their dwell time in specific areas.

F. Morris Water Maze

The Morris water maze (MWM) is a commonly used task for evaluating the spatial memory and learning ability of mice [25]. After the open field experiment, a 5-day water maze test (Days 29-33) was carried out. A circular pool (60 cm in diameter) was divided into four distinctively marked quadrants: northeast (NE), northwest (NW), southeast (SE) and southwest (SW). The pool was filled with water to a depth of 21 cm. Milk was added to make the colour difference between the mouse and the water surface more obvious. In the first four days, a platform (height=20 cm) was placed in the middle of the NE quadrant, and experiments were conducted four times a day, with an interval of no more than 10 minutes between successive experiments. The mice were slowly lowered into the pool from four directions; we ensured that the order of placement was not the same every day. The latency time and trajectory of the mice to find the platform were recorded. If the mouse did not find the platform within 60 s, it was guided to the platform and allowed to stay there for 15 s, and the latency was recorded as 60 s. After each experiment, the mice were dried and placed on a heating pad to keep warm. On the fifth day, the platform was removed, and a 120-s probe trial was performed. Performance was monitored with a video recording system (Basler, acA1280-60gm). The trajectory of the mice, the number of times they crossed the former platform location, the total distance travelled, and the dwell time in the quadrant previously containing the platform were quantitatively analysed.

G. Electrode Implantation and EEG Recordings

After the mouse was anaesthetized with 0.5% isoflurane, it was fixed on an adapter (ST-5ND-C, Stoelting Co., USA), the scalp was cut away, and a window was opened at the electrode implantation site using a cranial drill with a size of approximately 2 mm×2 mm (the coordinates of the centre of the 16-channel electrode (MWA-S16) were as follows: anteroposterior(AP) = −2 mm, mediolateral(ML) = 1 mm, dorsoventral(DV) = 1.5 mm) (Fig. 1a, right). A skull pin was implanted at the position of the mouse cerebellum, connecting the ground wire of the electrode. The electrodes were fixed on the heads of the mice using dental cement, and the mice were allowed to recover for one week. During electrode implantation, a temperature control device was used to keep the temperature of the mice at ∼37°C. The production of the EEG acquisition model in freely moving mice is not marked in the timeline of the experiment. EEG activity in freely moving mice was recorded with a multichannel data acquisition system (Apollo, Bio-Signal Technologies: McKinney, TX, USA) (Fig. 1a, middle). The electrode with 16 recording channels simultaneously recorded spikes and LFPs from the hippocampus. The raw data were collected during day CIS for 15 minutes with a 30 kHz sampling rate.

H. Relative Power and Cross-Frequency Coupling Analyses

All analyses were performed using MATLAB. LFP power spectral density (PSD) was calculated through the Welch estimate method (pwelch.m). The spectral power in the different frequency bands was obtained under the PSD curve, with a frequency resolution of 0.5 Hz. The relative power (RP) of delta (1.5-5 Hz), theta (5-10 Hz), gamma (30-90 Hz) and epsilon (90-190 Hz) were calculated based on PSD ($RP=Power\_/Power_{0-200Hz}$). For the analysis of the cross-frequency phase-amplitude coupling (CFC-PAC) [28], [29], the PAC was calculated by computing the phase-locked value index for the phase of lower frequencies (delta and theta) with respect to the lower frequencies phase of the higher frequencies (gamma and epsilon) amplitude. The amplitude and phase components were obtained by using a Hilbert transform.

I. Spike Sorting and Firing Rate Analysis

Spikes were extracted from high-frequency signals (>300 Hz). Blackrock Offline Spike Sorter software (1.2.0, Blackrock, USA) was used to classify the collected spikes into pyramidal neurons and interneurons based on principal component analysis [30], [31] and the K-means algorithm [32]. Moreover, spike durations were also used to distinguish pyramidal neurons (PN) (longer, 0.86 ± 0.17 ms) and interneurons (IN) (shorter, 0.43 ± 0.27 ms), which were used in our previous study [33], [34]. The interspike interval (ISI) histogram was generated, and its shape could also be used as a reference for the classification characteristics of the two types of neurons [35]. After spike sorting, the number of spikes per second from each of the two types of neurons was calculated during day CIS; this variable is called the firing rate (FR).

J. Detection of Theta Oscillations and Phase-Locked Firing Analysis

The theta oscillations of LFP were obtained digitally band-pass filtered from 5 to 10 Hz. The corresponding relationship between spike firing and the theta-filtered LFP was indicated by counting the mean FR at the corresponding time of LFP with 1 ms as the bin [36]. To evaluate the presence of phase locking, the phase was divided into 30 equal parts with the mean FR of the spike in the corresponding time, and Rayleigh's test for circular uniformity was performed to compute the significance ($p < 0.05$) of phase locking.

K. Statistical Analysis

All data are expressed as the mean ± SEM. Statistical analysis was performed using repeated measures two-way analysis of variance (ANOVA) with least significant difference post hoc test for multiple comparisons (GraphPad Prism Software and SPSS Software). Multiple comparisons of the theta phase-locking were conducted using the Rayleigh's test with the false discovery rate test. The level of statistical significance was set at a p value < 0.05.

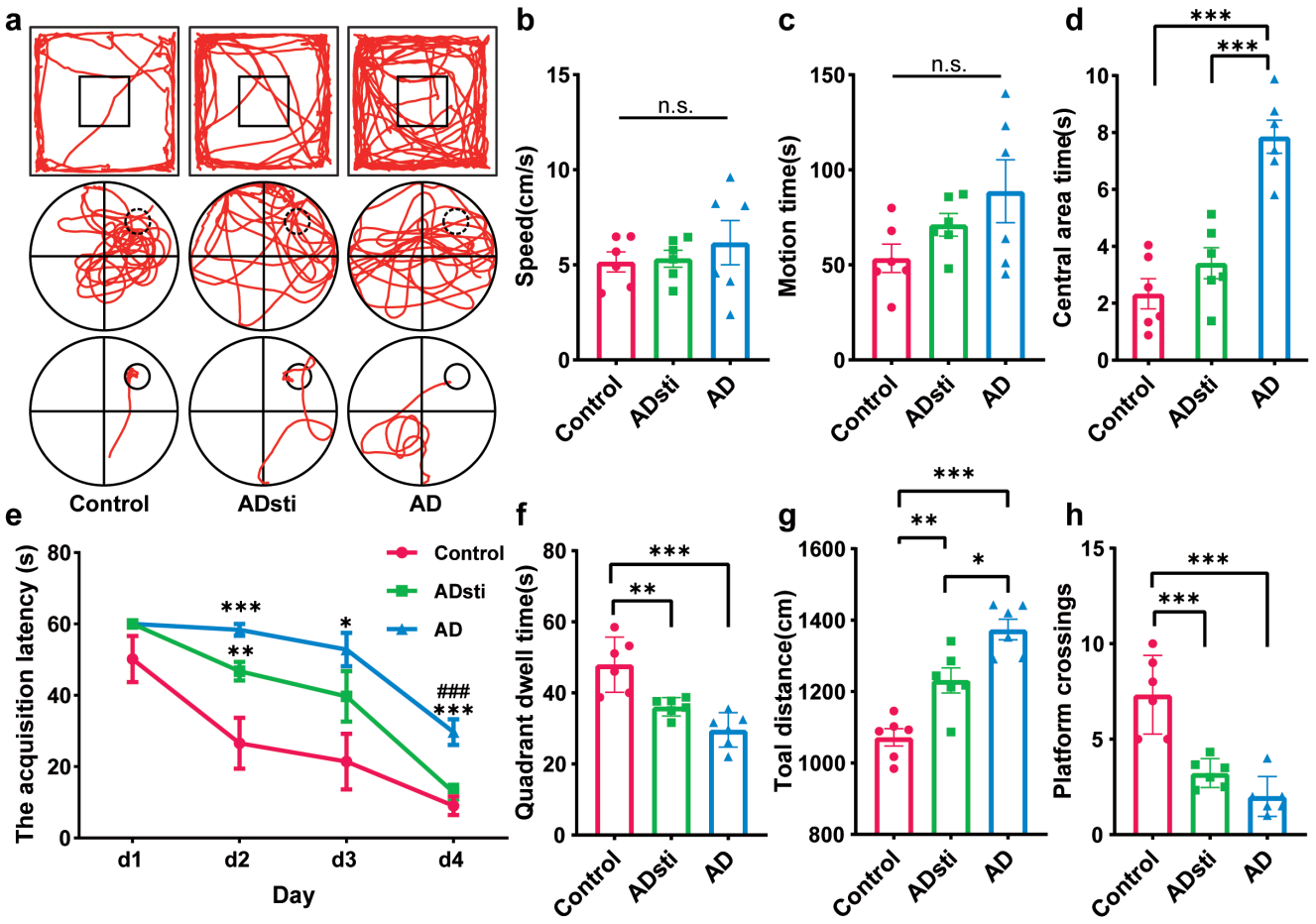

Fig. 2. Results of the open field (OF) and Morris water maze (MWM) tests. (a) Representative motion paths of control, ADsti, and AD group mice in the OF test (top) and on the fourth (with platform, bottom) and fifth days (without platform, middle) of the MWM test. (b-d) The speed, motion time and central area time in the OF test. (e-h) The acquisition latency, quadrant dwell time, total distance and platform crossings in the MWM test. Data are shown as the mean ± SEM for n=6 mice per group; in Figure 1e, *p<0.05, **p<0.01, ***p<0.001 vs. Control; #p<0.05, ##p<0.01, ###p<0.001; vs. ADsti.

III. Results

A. Effects of Ultrasound on Voluntary Movement, Anxiety Behaviour, Learning and Memory in APP/PS1 Mice

After ultrasonic stimulation, an open-field experiment was conducted on day 28 to explore the effects of voluntary movement and anxiety in mice. The results of movement time (Fig. 2b) and movement speed (Fig. 2c) of mice in each group showed that there was no significant difference in motor function between the early AD mouse model and normal mice. Figure 2a (upper) shows the movement track of the mouse, and the middle rectangular box is defined as the middle area. Figure 2d shows that the AD group stayed in the middle area longer than the control group ($p<0.001$), and the ADsti group stayed significantly lower than the AD group ($p<0.001$),which suggested that TUS can make the anxiety behaviour of AD mice close to that of the control group.

On days 29-33, we conducted a 5-day MWM test to explore the spatial learning and memory abilities of mice. Figure 2a (bottom, middle) shows the search strategy on the fourth day (fixed platform) and fifth day (removed platform). This trajectory shows that the ADsti and AD groups tended to scan-search, whereas the ADsti group had a simpler search strategy and the control group had a straightforward strategy. From 1 to 4 days, the latency of the three groups of mice gradually decreased, indicating that the memory formation ability of AD mice was healthy (Fig. 2e). There was no significant difference in latency between the three groups on the first day, and the latency of the AD group was significantly higher than that of the control group from the second day, while the latency of the ADsti group was lower than that of the AD group and was significantly lower than that of the AD group on the fourth day ($p<0.001$). There was no significant difference in latency between the ADsti group and the control group on the fourth day. After the platform was removed on the fifth day, the dwell time, total movement distance, and number of platform crossings of the three groups were calculated in the original platform quadrant. There were significant differences in the three indices between the AD and control groups ($p<0.001$). The residence time in the original platform quadrant and the number of platform crossings in the ADsti group were higher than those in the AD group, but there was no significant difference between the two groups, while the total movement distance in the ADsti group was significantly lower than that in the AD group ($p<0.05$). These results suggest that ultrasound can improve spatial memory and learning in AD mice.

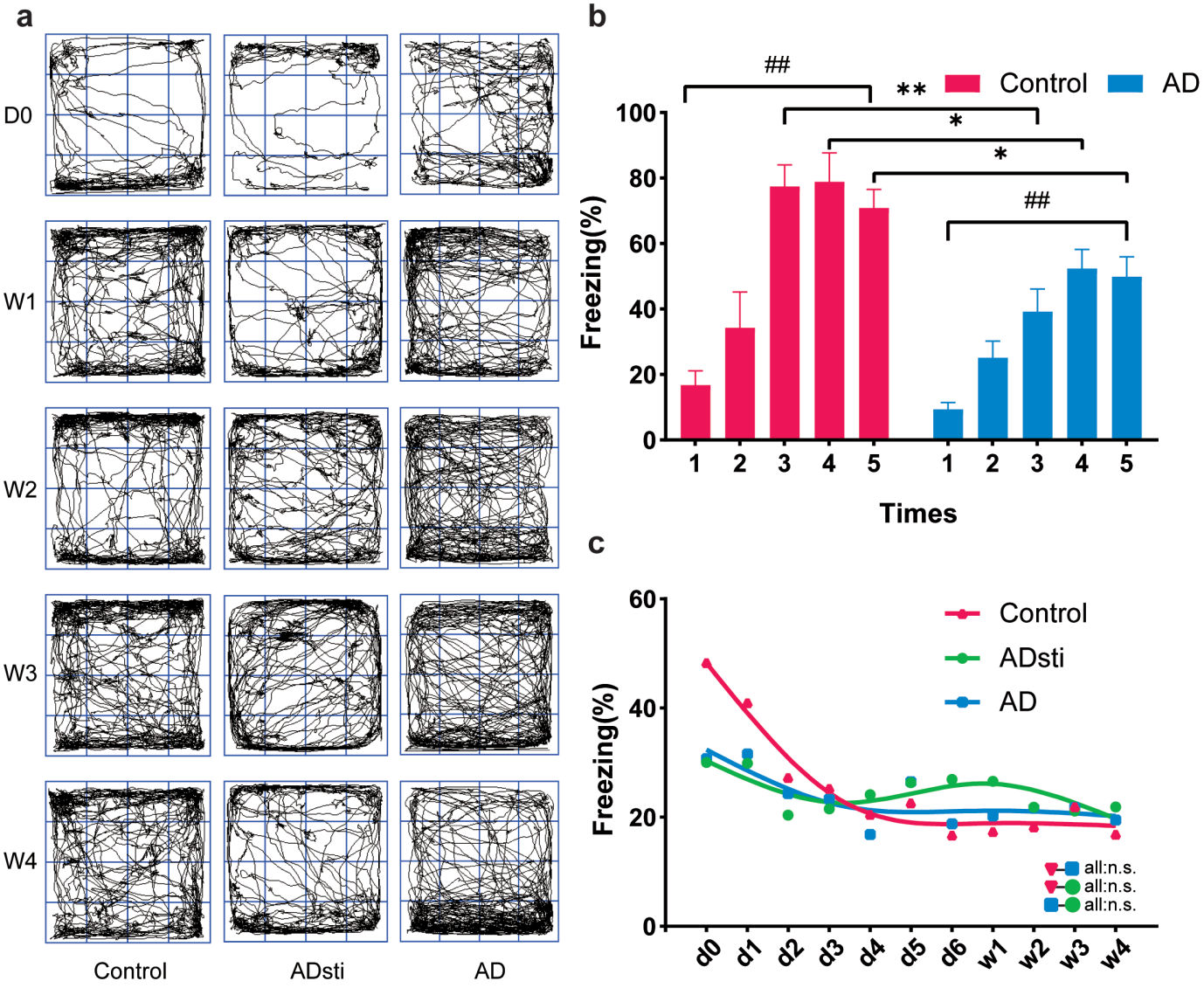

Fig. 3. Results of the fear conditioning(FC) test. (a) Representative motion paths of control, ADsti, and AD group mice at Day 0, Week 1, Week 2, Week 3, and Week 4. (b) Levels of freezing behaviour in the training stage. (c) Levels of freezing behaviour in the testing stage during day CIS. Data are shown as the mean ± SEM for n=6 mice per group.

B. Changes in Fear Memory in APP/PS1 Mice Under Ultrasound Stimulation

After the mice developed fear memory, we conducted the fear conditioning test during day CIS to observe the changes in fear memory in APP/PS1 mice under long-term ultrasound. Figure 3a shows a representative trajectory map. We used the immobility time ratio to characterize the degree of fear memory in mice. The mice were trained five times during the formation of fear memory. As the training times increased, the immobility time ratio of the mice increased, and the immobility time ratio after the fifth training was more than 5 times that of the first training($p<0.01$); therefore, we considered the establishment of fear memory in mice to be successful. The difference in the immobility time ratio between the AD group and the control group after the third training session was significant($p<0.05$) (Fig. 3b). During day CIS, the change in the immobility time ratio of mice under sound stimulation is shown in Figure 3c. The overall trend of the immobility time ratio of the three groups was all decreased, and there was no significant difference among the groups. However, the ADsti group had an increase in immobility time compared with rebound after 4 days of ultrasound stimulation and decreased to the same level as the AD and control groups after 28 days of stimulation. These results suggest that ultrasound may bring the short-term fear memory rebound in AD mice.

C. Analysis Results of Relative Power and Cross-Frequency Coupling in APP/PS1 Mice Under Ultrasound

In general, hippocampal oscillations are mainly concentrated in the theta and gamma bands, as abnormal phase-amplitude coupling (PAC) between these bands is associated with cognitive impairment [37], [38]. The delta (1.5-5 Hz) frequency band is a slow wave associated with memory consolidation [39], and the epsilon (90-190Hz) frequency band is a fast oscillation supporting memory consolidation that mediates the transfer of newly acquired hippocampal information to brain-wide circuits during waking and non-REM

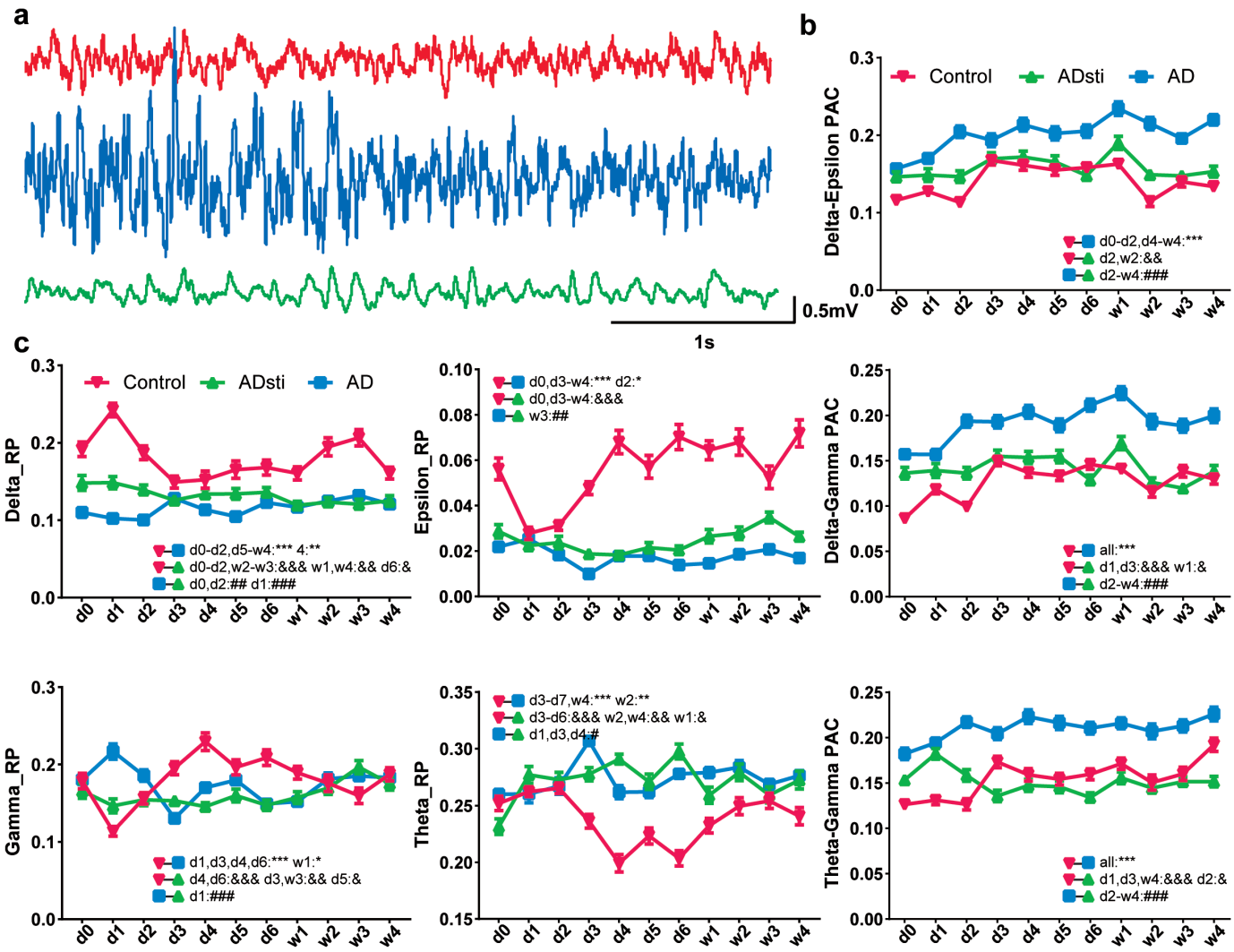

Fig. 4. Results of local field potential (LFP). (a) Representative LFP waveforms of Control, ADsti, and AD group mice in week 4. (b) The results of cross-frequency coupling (delta-epsilon, delta-gamma and theta-gamma) under ultrasound treatment during day CIS. (c) Relative power of different frequency ranges (delta, epsilon, gamma and theta) under ultrasound treatment during day CIS. Data are shown as the mean ± SEM for n=6 mice per group; *p<0.05, **p<0.01, ***p<0.001, Control vs. AD; &p<0.05, &&p<0.01, &&&p<0.001, Control vs. ADsti; #p<0.05, ##p<0.01, ###p<0.001, ADsti vs. AD. Abbreviations: PAC, Phase-amplitude coupling; RP,Relative power.

sleep [40], [41]. Then the four rhythms of LFP collected during day CIS were analysed. Figure 4a is a partial representative LFP waveform of three groups in week 4, and then we calculated the PAC of delta-epsilon, delta-gamma and theta-gamma, except for the PAC values of the delta-epsilon in D3-D6, the PAC values of the AD group were significantly greater than those of the Control group($p<0.001$), and there was a significant difference between the ADsti group and the AD group basically from the second day of ultrasound stimulation($p<0.001$) (Fig. 4b). Based on the change results of the cross frequency coupling(CFC) of the three rhythm pairs, we calculated the relative power of delta, epsilon, gamma and theta rhythms and found that overall, relative to the AD group, the relative power of delta and epsilon in the Control group were generally increased, whereas there were no significant differences in gamma or theta rhythms (Fig. 4c). At the same time, ultrasonic stimulation had no effect on the relative power of these four rhythms in AD mice, except that the relative power of epsilon in the ADsti group was greater than that in the AD group once at week 3 ($p<0.01$). These results suggest that ultrasound stimulation can improve the PAC of delta-epsilon, delta-gamma and theta-gamma and power imbalances of epsilon rhythm in AD mice.

D. Firing Rate and Phase-Locking Results of APP/PS1 Mice Under Ultrasonic Stimulation

Figure 5a shows the representative timestamps, interspike interval histograms and spike waveforms of the single spikes of the two types of neurons (IN, PN) after the spike classification of mice in each group at week 4. Among them, PN discharge is more concentrated, and this result is consistent with the research of single spikes by other scholars [42], [43]. Next, the firing rates of the two types of neurons were analysed, and the results showed that there was no significant difference in the firing rates of PN among the three groups(Fig. 5b, right). For IN, compared with the control, the discharge rate of AD developed from low on day 2 ($p<0.001$) to high on weeks 2 and 4 ($p<0.05$) (Fig. 5b, left).

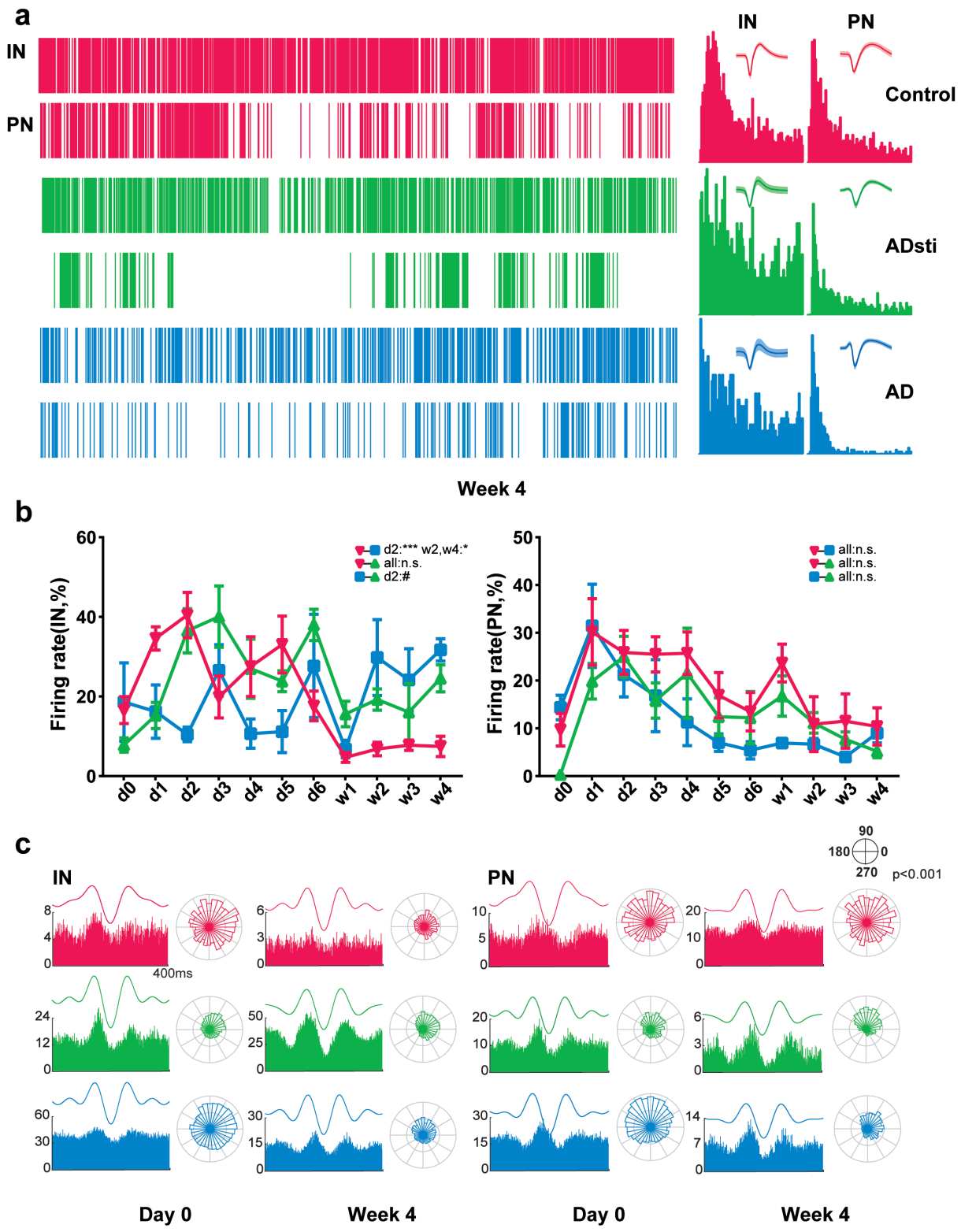

Fig. 5. Results of spikes in the hippocampus during ultrasound hippocampus stimulation. (a) Left: Representative single spike timestamps (interneurons, IN; and pyramidal neurons, PN) of control, ADsti, and AD group mice in week 4. Right: Corresponding interspike interval histograms (ISI) and spike waveforms. (b) The total firing rate on day CIS (left: INs; right: PNs). (c) Single spike firing, theta oscillation, and phase locking for single spike firing and theta oscillation on day 0 and week 4 (left: INs; right: PNs; Rayleigh's test, $p<0.001$). Data are shown as the mean ± SEM for n=6 mice per group; *p<0.05, **p<0.01, ***p<0.001, Control vs. AD; &p<0.05, &&p<0.01, &&&p<0.001, Control vs. ADsti; #p<0.05, ##p<0.01, ###p<0.001, ADsti vs. AD.

In the late ultrasonic stimulation period, although there was no significant difference between ADsti and other groups, the ADsti group was higher than the control group and lower than the AD group. These results suggest that ultrasound stimulation may weaken the excitability of IN neurons in AD mice.

Finally, we also analysed the theta-spike coupling of the single spikes of the two types of neurons. Figure 5c shows the average 400 ms theta rhythm segment of single spikes of the two representative types of neurons on day 0 and week 4, where the trough of the theta wave cycle is located at 200 ms. In addition, the average discharge rate over time during these 400 ms was calculated, and a polar coordinate diagram of a complete theta wave cycle where the trough was located at 200 ms was drawn. Both types of neurons in the three groups of mice were phase-locked by the Rayleigh's test ($p<0.001$). For IN, the spike releases of the Control group on day 0 and week 4 were all phase-locked near the peak of the theta wave and relatively less concentrated (∼270-90°); compared with the Control group, the spike emission in the AD group and ADsti group was phase-locked at the falling edge of the theta wave (∼0-90°). After 28 days of ultrasonic stimulation, the phase-locking phase angle of the ADsti group shifted to the peak (∼0-90°, more concentrated on 0°), while the AD group was more shifted to the trough (∼60-120°), and we found that the phasing results of the AD group and ADsti group were more concentrated. For PN, consistent with IN, compared to the control group (Day 0: ∼70-180°; Week 4: ∼330-150°), the spike discharge was more concentrated in the AD group (Day 0: ∼60-150°; Week 4: ∼0-90°) and ADsti group (Day 0: ∼30-110°; Week 4: ∼50-130°). After 28 days of ultrasonic stimulation, in week 4, the phase-locked phase angle of the AD group shifted to the peak, but there was no significant change in the ADsti group. The results showed that ultrasound stimulation can suppress or improve the deviation of phase-locked angles in the AD mice with the course of the disease.

IV. Discussion

In this study, we applied a 28-day course of low-intensity TUS to the hippocampus of an AD mouse model and conducted memory-related behavioural studies. We found that the voluntary movement ability and memory formation ability of the early AD mouse model have not undergone significant pathological changes, but the spatial memory and learning ability and sensitivity to sensations, including anxiety and fear, have all decreased significantly. Interestingly, ultrasound stimulation improves spatial memory and learning and restores some sensory sensitivity in early AD mice. The motor ability of AD mice has no significant difference between the Control group, AD group, and ADsti group. In addition, the anxiety level of AD mice is significantly higher than that of the normal mice. These results indicate that TUS can significantly improve the reduction of anxiety levels in AD mice. The results of the probe trials in the MWM were not significant and the latency time of the ADsti group was significantly lower than that of the AD group, indicating that ultrasound stimulation improved the spatial memory and learning ability of AD mice. It demonstrates that the therapeutic effect was acquisition. After establishing a fear memory of sound stimulation in the first two days, the three groups of mice used the same experimental mode and there was no significant difference between the three groups in the results of freezing behavior. There is no significant statistics difference in the immobility time ratio between the control group and other groups. To further investigate the physiological mechanism behind the improvement of behaviour by ultrasound stimulation, we conducted a correlation analysis of neural oscillations and found some neurophysiological basis for functional improvement.

On day CIS, 16-channel electrodes were used to collect LFPs and spikes in the hippocampus of mice, and it was found that early AD mice had partial rhythm imbalance and inter-rhythm phase-amplitude coupling disorder. Recent studies have shown that theta-gamma coupling correlates with working memory performance [44], [45]. Impairment of theta-gamma coupling followed by memory impairment was reported by Goodman et al. in 2018 [46]. Through LFP analysis, our results suggest that AD mice develop partial rhythmic power imbalances. The relative power of delta and epsilon in AD mice is low, and the epsilon power of AD mice tends to increase after ultrasonic stimulation, but perhaps the gamma and theta rhythms of the early AD mouse model have not yet been abnormal. Theta-gamma coupling has also been considered a biomarker to assess generalized EEG suppression [47]. In our study, phase-amplitude coupling disorder among rhythms appeared in AD mice, and ultrasonic stimulation improved the PAC of delta-epsilon, delta-gamma and theta-gamma. However, the four rhythmic powers of AD mice were not completely unbalanced, but their PAC corresponding to delta-epsilon, delta-gamma and theta-gamma increased, and the mechanism needs to be further explored. Little work has been done on neuronal firing in young APP/PS1 mice, which we partially analysed.

The spikes collected by day CIS were classified into two types of neurons (IN, PN), and long-term accumulation of ultrasonic stimulation decreased the excitability of IN in AD mice but did not affect PN. The IN neuron firing rate of mice in the control group significantly on the first to fourth weeks was lower than that on the first to sixth days. As shown in Figure S1(c), there was no significant difference for the IN-firing rate between d0 and w4 in the control group. Similar to IN, as shown in Figure S1(d), there was no significant difference for the PN-firing rate of mice between the mean of d0-d6 and w4 in each group. As shown in Figure S2(d-f), the firing rates of IN neurons collected every week from w1 to w4 were relatively stable with no significant difference. It indicates that the statistical results between different groups in the late stage of ultrasound stimulation were meaningful. As we know, the stability of spatial memory is related to interneurons (INs) and pyramidal neurons (PNs) with different functional ranges. The plasticity of INs makes the positional cells within CA1 more stable, among which positional cells are PNs that are extremely important for spatial memory, and INs may be the key to stable memory [48]. The possible reasons for the different results of INs and PNs may be the direct effect of TUS on two types of neurons and the interaction between the two types of neurons. Consistent with previous studies, the discharge of PN was more concentrated [42], [43]. We speculate that the development of AD is related to excessive excitation of IN and does not have obvious effects on PNs during early AD. Theta-spike coupling analysis was

performed on the single spikes of the two types of neurons. The results showed that the phase locking of the two types of neurons in AD mice was more concentrated, and the phase locking angles of IN and PN in AD mice shifted with the course of the disease, while prolonged TUS suppressed or ameliorated this shift. We speculate that the development of AD will be accompanied by a phase angle imbalance between theta rhythm and spike firing and that spike firing in AD mice will be more dependent on specific phases.

Previous work has shown that ultrasound stimulation can modulate memory-related neuronal firing as well as promote dendritic spine growth and reduce dendritic spine elimination [49], [50]. In our work, we found that ultrasound stimulation can improve the memory ability of AD mice and modulate action potentials and LFPs in the hippocampus. Furthermore, previous studies have also shown that ultrasound stimulation induces neuronal firing activity by acting on mechanosensitive ion channels (Piezo1) [51] or potassium channels (TRAAK) [52] et al. Therefore, the potential mechanism by which our ultrasound stimulation improves AD behavior may be that ultrasound causes neuronal discharges by acting on ion channels. A large number of neuronal discharges alter the LFPs coding in the hippocampus, thereby improving the memory behavior of AD mice. We will conduct further in-depth research in our next work.

Previous studies have reported that TUS modulates neural activity through non-specific auditory responses [53], [54]. To evaluate the effect of non-specific auditory responses in our experiments, six AD mice were stimulated with a specific ultrasound (trapezoidal pulses) that have been proved with no auditory response in TUS [55]. The results shown in Figure S1 indicate that the modulation effect of TUS on AD is not due to auditory effects. The results shown in Figure S2(a-c) indicate that some features of the AD group changed as function of progression time.In addition, the ELISA analysis results shown in Figure S3 indicate that 28 days of ultrasound stimulation can significantly reduce the expression of Aβ and Tau protein (hallmarks of AD) in the hippocampus and cortex of AD mice.

Considering the safety of long-term low-intensity TUS of 15 minutes per day for 28 days, we provide the following explanations. First, the ultrasound intensity we selected conforms to the clinical use standard of the FDA [16]. Second, the parameters we chose are consistent with the ultrasound parameters of the Taiwanese team, and their results show that ultrasound stimulation will not cause damage to the brain tissue of mice [56], [57].

V. Limitations

The shortcomings of this study are as follows: 1) The parameters selected for ultrasonic stimulation are single, not necessarily the best parameters. 2) Due to the limitations of the electrodes, we only collected EEG from the hippocampus and did not collect multiple brain regions. It is impossible to analyse and study neural oscillations across brain regions. 3) AD is a chronic disease, and it is uncertain whether the selected stimulation cycle (28 days) is the best treatment course. 4) The experimental design does not collect daily LFPs and spikes under ultrasonic stimulation, and the timely response to ultrasound stimulation creates a gap. In future research, we will compensate for the shortcomings of the present study as follows. First, we will improve the design of electrodes and conduct research on neural oscillations across brain regions. Then, we will collect the electrical signal under ultrasonic stimulation to study the timely response of ultrasonic stimulation and find the best stimulation cycle treatment course. Finally, we will conduct multiparameter stimulation experiments to find the best stimulation parameters.

VI. Conclusion

In summary, we used long-term low-intensity TUS to act on the hippocampus of AD mice and simultaneously recorded LFPs and spikes. Based on the improvement in AD-related behavioural measures after ultrasonic stimulation, we analysed LFPs and spikes; the results showed that ultrasonic stimulation can improve some rhythm imbalances and phase-amplitude coupling disorders of some rhythm pairs in AD mice. Moreover, TUS can attenuate the excitability of IN in AD mice and inhibit or improve the phase-locked phase angle offset of theta rhythm and spike firing.These results provide a basis for ultrasound therapy of AD.

Conflict of Interest

The author(s) declare no potential conflicts of interest with respect to the research, authorship, and/or publication of this article.

References

[1] M. Nafea, M. Elharoun, M. M. Abd-Alhaseeb, and M. W. Helmy, "Leflunomide abrogates neuroinflammatory changes in a rat model of Alzheimer's disease: The role of TNF-α/NF-κB/IL-1β axis inhibition," *Naunyn-Schmiedeberg's Arch. Pharmacol.*, vol. 396, no. 3, pp. 485–498, Mar. 2023.

[2] S. Zhou and G. Huang, "The biological activities of butyrylcholinesterase inhibitors," *Biomed. Pharmacotherapy*, vol. 146, Feb. 2022, Art. no. 112556.

[3] T. Tan et al., "Low-frequency (1 Hz) repetitive transcranial magnetic stimulation (rTMS) reverses Aβ(1-42)-mediated memory deficits in rats," *Exp. Gerontol.*, vol. 48, no. 8, pp. 786–794, Aug. 2013.

[4] P. Turriziani et al., "Low-frequency repetitive transcranial magnetic stimulation of the right dorsolateral prefrontal cortex enhances recognition memory in Alzheimer's disease," *J. Alzheimer's Disease*, vol. 72, no. 2, pp. 613–622, Nov. 2019.

[5] E. M. Khedr et al., "A double-blind randomized clinical trial on the efficacy of cortical direct current stimulation for the treatment of Alzheimer's disease," *Frontiers Aging Neurosci.*, vol. 6, p. 275, Oct. 2014.

[6] K. Yu, X. Niu, and B. He, "Neuromodulation management of chronic neuropathic pain in the central nervous system," *Adv. Funct. Mater.*, vol. 30, no. 37, Sep. 2020, Art. no. 1908999.

[7] Y. Yuan, Z. Wang, M. Liu, and S. Shoham, "Cortical hemodynamic responses induced by low-intensity transcranial ultrasound stimulation of mouse cortex," *NeuroImage*, vol. 211, May 2020, Art. no. 116597.

[8] A. Bystritsky et al., "A review of low-intensity focused ultrasound pulsation," *Brain Stimulation*, vol. 4, no. 3, pp. 125–136, Jul. 2011.

[9] M. Fini and W. J. Tyler, "Transcranial focused ultrasound: A new tool for non-invasive neuromodulation," *Int. Rev. Psychiatry*, vol. 29, no. 2, pp. 168–177, Apr. 2017.

[10] E. Landhuis, "Ultrasound for the brain," *Nature*, vol. 551, no. 7679, pp. 257–259, 7679.

[11] X. Niu, K. Yu, and B. He, "On the neuromodulatory pathways of the in vivo brain by means of transcranial focused ultrasound," *Current Opinion Biomed. Eng.*, vol. 8, pp. 61–69, Dec. 2018.

[12] Y. Yuan, Z. Wang, X. Wang, J. Yan, M. Liu, and X. Li, "Low-intensity pulsed ultrasound stimulation induces coupling between ripple neural activity and hemodynamics in the mouse visual cortex," *Cerebral Cortex*, vol. 29, no. 7, pp. 3220–3223, Jul. 2019.

[13] D. Dalecki, "Mechanical bioeffects of ultrasound," *Annu. Rev. Biomed. Eng.*, vol. 6, no. 1, pp. 229–248, Aug. 2004.

[14] A. Fomenko, C. Neudorfer, R. F. Dallapiazza, S. K. Kalia, and A. M. Lozano, "Low-intensity ultrasound neuromodulation: An overview of mechanisms and emerging human applications," *Brain Stimulation*, vol. 11, no. 6, pp. 1209–1217, Nov. 2018.

[15] M. Park et al., "Effects of transcranial ultrasound stimulation pulsed at 40 Hz on β plaques and brain rhythms in 5XFAD mice," *Transl. Neurodegener.*, vol. 10, no. 1, p. 48, 2021.

[16] G. Leinenga et al., "Transcriptional signature in microglia isolated from an Alzheimer's disease mouse model treated with scanning ultrasound," *Bioeng. Transl. Med.*, vol. 8, no. 1, Jan. 2023, Art. no. e10329.

[17] W.-T. Lin, R.-C. Chen, W.-W. Lu, S.-H. Liu, and F.-Y. Yang, "Protective effects of low-intensity pulsed ultrasound on aluminum-induced cerebral damage in Alzheimer's disease rat model," *Sci. Rep.*, vol. 5, no. 1, p. 9671, Apr. 2015.

[18] C.-Z. Yang et al., "Neuroprotective effect of astragalin via activating PI3K/Akt-mTOR-mediated autophagy on APP/PS1 mice," *Cell Death Discovery*, vol. 9, no. 1, p. 15, Jan. 2023.

[19] Y.-Y. Wang et al., "Long-term voluntary exercise inhibited AGE/RAGE and microglial activation and reduced the loss of dendritic spines in the hippocampi of APP/PS1 transgenic mice," *Experim. Neurol.*, vol. 363, May 2023, Art. no. 114371.

[20] K. Li, Y. Jiang, G. Li, T. Liu, and Z. Yang, "Novel multitarget directed tacrine hybrids as anti-Alzheimer's compounds improved synaptic plasticity and cognitive impairment in APP/PS1 transgenic mice," *ACS Chem. Neurosci.*, vol. 11, no. 24, pp. 4316–4328, Dec. 2020.

[21] J. J. Gallagher, A. M. Minogue, and M. A. Lynch, "Impaired performance of female APP/PS1 mice in the Morris water maze is coupled with increased aβ accumulation and microglial activation," *Neurodegenerative Diseases*, vol. 11, no. 1, pp. 33–41, 2013.

[22] K. Richetin, P. Petsophonsakul, L. Roybon, B. P. Guiard, and C. Rampon, "Differential alteration of hippocampal function and plasticity in females and males of the APPxPS1 mouse model of Alzheimer's disease," *Neurobiol. Aging*, vol. 57, pp. 220–231, Sep. 2017.

[23] J. B. Aimone, W. Deng, and F. H. Gage, "Resolving new memories: A critical look at the dentate gyrus, adult neurogenesis, and pattern separation," *Neuron*, vol. 70, no. 4, pp. 589–596, May 2011.

[24] E. Kumari, Y. Shang, Z. Cheng, and T. Zhang, "U1 snRNA overexpression affects neural oscillations and short-term memory deficits in mice," *Cognit. Neurodyn.*, vol. 13, no. 4, pp. 313–323, Mar. 2019.

[25] S.-L. Huang, C.-W. Chang, Y.-H. Lee, and F.-Y. Yang, "Protective effect of low-intensity pulsed ultrasound on memory impairment and brain damage in a rat model of vascular dementia," *Radiology*, vol. 282, no. 1, pp. 113–122, Jan. 2017.

[26] J. P. Johansen, C. K. Cain, L. E. Ostroff, and J. E. LeDoux, "Molecular mechanisms of fear learning and memory," *Cell*, vol. 147, no. 4, p. 948, Nov. 2011.

[27] Y. Yuan, Z. Zhao, Z. Wang, X. Wang, J. Yan, and X. Li, "The effect of low-intensity transcranial ultrasound stimulation on behavior in a mouse model of Parkinson's disease induced by MPTP," *IEEE Trans. Neural Syst. Rehabil. Eng.*, vol. 28, no. 4, pp. 1017–1021, Apr. 2020.

[28] B. Voytek, M. D'Esposito, N. Crone, and R. T. Knight, "A method for event-related phase/amplitude coupling," *NeuroImage*, vol. 64, pp. 416–424, Jan. 2013.

[29] A. Leparulo, M. Bisio, N. Redolfi, T. Pozzan, S. Vassanelli, and C. Fasolato, "Accelerated aging characterizes the early stage of Alzheimer's disease," *Cells*, vol. 11, no. 2, p. 238, Jan. 2022.

[30] M. Lewicki, "A review of methods for spike sorting: The detection and classification of neural action potentials," *Network: Comput. Neural Syst.*, vol. 9, no. 4, pp. R53–R78, Nov. 1998.

[31] J. Hu, J. Si, B. P. Olson, and J. He, "Feature detection in motor cortical spikes by principal component analysis," *IEEE Trans. Neural Syst. Rehabil. Eng.*, vol. 13, no. 3, pp. 256–262, Sep. 2005.

[32] E. Chah, V. Hok, A. Della-Chiesa, J. J. H. Miller, S. M. O'Mara, and R. B. Reilly, "Automated spike sorting algorithmbased on Laplacian eigenmaps and k-means clustering," *J. Neural Eng.*, vol. 8, no. 1, Feb. 2011, Art. no. 016006.

[33] P. Barthó, H. Hirase, L. Monconduit, M. Zugaro, K. D. Harris, and G. Buzsáki, "Characterization of neocortical principal cells and interneurons by network interactions and extracellular features," *J. Neurophysiol.*, vol. 92, no. 1, pp. 600–608, Jul. 2004.

[34] L. Zhang et al., "Hippocampal theta-driving cells revealed by Granger causality," *Hippocampus*, vol. 22, no. 8, pp. 1781–1793, Aug. 2012.

[35] T. Takekawa, Y. Isomura, and T. Fukai, "Accurate spike sorting for multi-unit recordings," *Eur. J. Neurosci.*, vol. 31, no. 2, pp. 263–272, Jan. 2010.

[36] T. Klausberger, L. F. Márton, A. Baude, J. D. B. Roberts, P. J. Magill, and P. Somogyi, "Spike timing of dendrite-targeting bistratified cells during hippocampal network oscillations in vivo," *Nature Neurosci.*, vol. 7, no. 1, pp. 41–47, Jan. 2004.

[37] U. Rutishauser, I. B. Ross, A. N. Mamelak, and E. M. Schuman, "Human memory strength is predicted by theta-frequency phase-locking of single neurons," *Nature*, vol. 464, no. 7290, pp. 903–907, Apr. 2010.

[38] R. Goutagny et al., "Alterations in hippocampal network oscillations and theta-gamma coupling arise before Aβ overproduction in a mouse model of Alzheimer's disease," *Eur. J. Neurosci.*, vol. 37, no. 12, pp. 1896–1902, Jun. 2013.

[39] J. Kim, T. Gulati, and K. Ganguly, "Competing roles of slow oscillations and delta waves in memory consolidation versus forgetting," *Cell*, vol. 179, no. 2, pp. 514–526, Oct. 2019.

[40] M. Penttonen and G. Buzsáki, "Natural logarithmic relationship between brain oscillators," *Thalamus Rel. Syst.*, vol. 2, no. 2, p. 145, Apr. 2003.

[41] G. Buzsáki, "Hippocampal sharp wave-ripple: A cognitive biomarker for episodic memory and planning," *Hippocampus*, vol. 25, no. 10, pp. 1073–1188, Oct. 2015.

[42] X. Wang, J. Yan, H. Zhang, and Y. Yuan, "Ultrasonic thalamic stimulation modulates neural activity of thalamus and motor cortex in the mouse," *J. Neural Eng.*, vol. 18, no. 6, Dec. 2021, Art. no. 066037.

[43] X. Wang, Y. Zhang, K. Zhang, and Y. Yuan, "Influence of behavioral state on the neuromodulatory effect of low-intensity transcranial ultrasound stimulation on hippocampal CA1 in mouse," *NeuroImage*, vol. 241, Nov. 2021, Art. no. 118441.

[44] J. E. Lisman and O. Jensen, "The theta-gamma neural code," *Neuron*, vol. 77, no. 6, pp. 1002–1016, Mar. 2013.

[45] T. K. Rajji, R. Zomorrodi, M. S. Barr, D. M. Blumberger, B. H. Mulsant, and Z. J. Daskalakis, "Ordering information in working memory and modulation of gamma by theta oscillations in humans," *Cerebral Cortex*, vol. 27, Jan. 2016, Art. no. bhv326.

[46] M. S. Goodman et al., "Theta-gamma coupling and working memory in Alzheimer's dementia and mild cognitive impairment," *Frontiers Aging Neurosci.*, vol. 10, p. 101, Jan. 2018.

[47] V. Grigorovsky et al., "Delta-gamma phase-amplitude coupling as a biomarker of postictal generalized EEG suppression," *Brain Commun.*, vol. 2, no. 2, Jul. 2020, Art. no. fcaa182.

[48] M. Udakis, V. Pedrosa, S. E. L. Chamberlain, C. Clopath, and J. R. Mellor, "Interneuron-specific plasticity at parvalbumin and somatostatin inhibitory synapses onto CA1 pyramidal neurons shapes hippocampal output," *Nature Commun.*, vol. 11, no. 1, p. 4395, Sep. 2020.

[49] B. D. Boros, K. M. Greathouse, M. Gearing, and J. H. Herskowitz, "Dendritic spine remodeling accompanies Alzheimer's disease pathology and genetic susceptibility in cognitively normal aging," *Neurobiol. Aging*, vol. 73, pp. 92–103, Jan. 2019.

[50] X. Huang et al., "Transcranial low-intensity pulsed ultrasound modulates structural and functional synaptic plasticity in rat hippocampus," *IEEE Trans. Ultrason., Ferroelectr., Freq. Control*, vol. 66, no. 5, pp. 930–938, May 2019.

[51] J. Zhu et al., "The mechanosensitive ion channel Piezo1 contributes to ultrasound neuromodulation," *Proc. Nat. Acad. Sci. USA*, vol. 120, no. 18, May 2023, Art. no. e2300291120.

[52] B. Sorum, R. A. Rietmeijer, K. Gopakumar, H. Adesnik, and S. G. Brohawn, "Ultrasound activates mechanosensitive TRAAK k + channels through the lipid membrane," *Proc. Nat. Acad. Sci. USA*, vol. 118, no. 6, Feb. 2021, Art. no. e200698011.

[53] H. Guo et al., "Ultrasound produces extensive brain activation via a cochlear pathway," *Neuron*, vol. 98, no. 5, pp. 1020–1030, Jun. 2018.

[54] T. Sato, M. G. Shapiro, and D. Y. Tsao, "Ultrasonic neuromodulation causes widespread cortical activation via an indirect auditory mechanism," *Neuron*, vol. 98, no. 5, pp. 1031–1041, Jun. 2018.

[55] M. Mohammadjavadi, P. P. Ye, A. Xia, J. Brown, G. Popelka, and K. B. Pauly, "Elimination of peripheral auditory pathway activation does not affect motor responses from ultrasound neuromodulation," *Brain Stimulation*, vol. 12, no. 4, pp. 901–910, Jul. 2019.

[56] D. Zhang et al., "Antidepressant-like effect of low-intensity transcranial ultrasound stimulation," *IEEE Trans. Biomed. Eng.*, vol. 66, no. 2, pp. 411–420, Feb. 2019.

[57] W.-S. Su, C.-H. Wu, S.-F. Chen, and F.-Y. Yang, "Low-intensity pulsed ultrasound improves behavioral and histological outcomes after experimental traumatic brain injury," *Sci. Rep.*, vol. 7, no. 1, p. 15524, Nov. 2017.